Solid State Ionics 293 (2016) 77–84

Contents lists available at ScienceDirect

Solid State Ionics

journal homepage: www.elsevier.com/locate/ssi

Effect of lithium content on spinel phase evolution in the composite material $Li_xNi_{0.25}Co_{0.10}Mn_{0.65}O_{(3.4\ +\ x)\ /\ 2}$ $(0.8 \le x \le 1.6)$ for Li-ion batteries

Byungjin Choi [a], Jayhyok Song [b], Donghee Yeon [a], Jung-Hwa Kim [c], SeongYoung Park [c], Hyoun-Ee Kim [d], Jin-Hwan Park [a], Seokgwang Doo [a], Kwangjin Park [a,*]

[a] Energy Lab, Samsung Advanced Institute of Technology SAIT, Samsung Electronics Co., Ltd., Electronic Materials Research Complex, 130, Samsung-ro, Yongtong-gu, Suwon-si, Gyeonggi-do 16678, Republic of Korea
[b] Platform 2 team, Samsung SDI, Electronic Materials Research Complex, 130, Samsung-ro, Yongtong-gu, Suwon-si, Gyeonggi-do 16678, Republic of Korea
[c] Analytical Engineering group, Samsung Advanced Institute of Technology SAIT, Samsung Electronics Co., Ltd., Electronic Materials Research Complex, 130, Samsung-ro, Yongtong-gu, Suwon-si, Gyeonggi-do 16678, Republic of Korea
[d] Department of Materials Science and Engineering, Seoul National University, 1 Gwanak-ro, Gwanak-gu, Seoul 08826, Republic of Korea

ARTICLE INFO

Article history:
Received 18 May 2016
Received in revised form 10 June 2016
Accepted 10 June 2016
Available online 29 June 2016

Keywords:
Li-ion batteries
Lithium-rich oxides
Spinel structure
Co segregation
Li_2MnO_3

ABSTRACT

The composite material $Li_xNi_{0.25}Co_{0.10}Mn_{0.65}O_{(3.4\ +\ x)\ /\ 2}$ (x = 1.6, 1.4, 1.2, 1.0, 0.8) were synthesized and characterized for their structural, morphological, and performance as cathode materials in Li-ion batteries. The Rietveld refinement results indicate the presence of two phases at high lithium levels (x = 1.6 and 1.4): Li_2MnO_3 ($C2/m$) and $LiMO_2$ (***M***=Ni, Co, Mn) ($R\bar{3}m$); the latter contains Ni^{2+} and Ni^{3+}. At low lithium levels (x = 1.2, 1.0, and 0.8) an additional spinel phase LiM_2O_4 ($Fd\bar{3}m$) emerges, which is known to affect the electrochemical performance of the oxide. Structural analysis reveals that the spinel phase contains mixed transition metals Ni, Co, and Mn as $[Li^+,Co^{2+}][Ni^{2+},Co^{3+},Mn^{4+}]_2O_4$. A low lithium level is found to induce primary particle growth, as well as Co and Ni segregation within the secondary particles. These results are expected to contribute to material optimization and commercialization of lithium-rich oxide cathodes.

1. Introduction

The demand for Li-ion batteries (LIBs) has increased rapidly owing to their relatively high energy density and design flexibility. LIBs are attractive energy sources for applications ranging from mobile devices to large-scale products such as electric vehicles (EV) and energy-storage systems (ESS) [1–5]. However, the limited capacities from typical cathode materials such as $LiCoO_2$ and $LiMn_2O_4$ cannot satisfy the high energy density requirements for high-power LIBs used in EV and hybrid electric vehicles (HEV). Recently, lithium-rich layered oxide cathode materials, referred to as over-lithiated layered oxides (OLO) in the composite system $Li_2MnO_3 \cdot LiMO_2$ (***M***=Ni, Co, Mn), have shown capacities exceeding 250 mAh/g at high operating voltages (>3.5 V vs. Li/Li^+). However, lithium-rich oxide cathodes have several major drawbacks, including capacity loss during the first cycle, poor rate capability, and decreased cyclic performance [4,5]. Various approaches, such as surface modification and composition change including doping, have been used to overcome these problems [6]. Surface modification was used to block side reactions between the electrolyte and cathode at high voltage, and suppress phase changes during the cycle [7–10]. Others have focused on optimizing the composition to reduce transition metal migration during cycling in order to maintain the high capacity (>250 mAh/g) [11–14].

After screening various compositions, our research group has focused on the cobalt-containing $Li_{1.40}Ni_{0.25}Co_{0.10}Mn_{0.65}O_{2.40}$ "baseline" composition for EV applications [15]. Similar compositions have been studied by other groups and have been demonstrated to show promising performance [5,11–14,16–20]. However, a systematic study of the structure and phase evolution in these compositions is still lacking, [4,5,11–14] even though compositions with only Ni and Mn transition metals have been investigated extensively [1,21–25].

The addition of cobalt to lithium-rich oxides induces structural and morphological changes, especially in the spinel phase formation [4,5,11–14,16–20]. In the "layered-layered-spinel ($Li_2MnO_3 \cdot LiMO_2 \cdot LiM_xMn_{2-x}O_4$(***M***=Ni, Co, Mn))" composite structure, the initially embedded spinel phase has been shown to improve the voltage decay by stabilizing the "layered-layered ($Li_2MnO_3 \cdot LiMO_2$

* Corresponding author.
E-mail addresses: bj10.choi@samsung.com (B. Choi), jayhyok.song@samsung.com (J. Song), donghee.yeon@samsung.com (D. Yeon), jh1179.kim@samsung.com (J.-H. Kim), sydra.park@samsung.com (S. Park), kimhe@snu.ac.kr (H.-E. Kim), jin.h.park@samsung.com (J.-H. Park), sgdoo@samsung.com (S. Doo), ydmj79@gmail.com (K. Park).

http://dx.doi.org/10.1016/j.ssi.2016.06.012
0167-2738/

(***M***=Ni, Co, Mn))" composite [26,27]. The reported spinel phase in lithium-rich oxide are $LiMn_2O_4$ and $LiNi_{0.5}Mn_{1.5}O_4$ [21,23,26,28,29]. When cobalt is included, it is important to identify the spinel structure and composition, including the mixed transition metal spinel phase [30,31].

This work investigates the structural, morphological, and electrochemical performance changes in $Li_xNi_{0.25}Co_{0.10}Mn_{0.65}O_{(3.4\ +\ x)\ /\ 2}$ (x = 1.6, 1.4, 1.2, 1.0, 0.8). For brevity, they may be referred to as $Li_{1.60}$ …$Li_{0.80}$ throughout the rest of the article. The analytical methods used here include high-resolution powder diffractometry (HRPD), scanning electron microscope (SEM), transmission electron microscope (TEM), X-ray absorption near edge structure (XANES), extended X-ray absorption fine structure (EXAFS), and electron probe microscopic analysis (EPMA).

2. Experimental

2.1. Synthesis

The $Ni_{0.25}Co_{0.10}Mn_{0.65}(OH)_2$ precursor was prepared through a hydroxide co-precipitation process. Proper amounts of $NiSO_4 \cdot 6H_2O$, $CoSO_4 \cdot 7H_2O$, and $MnSO_4 \cdot H_2O$ were stirred in deionized water to form a homogeneous solution. The solution was chelated using NH_4OH and precipitated with NaOH. The co-precipitated $Ni_{0.25}Co_{0.10}Mn_{0.65}(OH)_2$ after drying was mixed with Li_2CO_3 to form the composite material with the average composition $Li_xNi_{0.25}Co_{0.10}Mn_{0.65}O_{(3.4\ +\ x)\ /\ 2}$ (x = 1.6, 1.4, 1.2, 1.0, 0.8) [16,23,32]. Their specific formulae are as follows:

$Li_{1.60}Ni_{0.25}Co_{0.10}Mn_{0.65}O_{2.50}$ (or $Li_{1.231}Ni_{0.192}Co_{0.077}Mn_{0.500}O_2$)

$Li_{1.40}Ni_{0.25}Co_{0.10}Mn_{0.65}O_{2.40}$ (or $Li_{1.167}Ni_{0.208}Co_{0.084}Mn_{0.542}O_2$)
$Li_{1.20}Ni_{0.25}Co_{0.10}Mn_{0.65}O_{2.30}$ (or $Li_{1.091}Ni_{0.227}Co_{0.091}Mn_{0.591}O_2$)
$Li_{1.00}Ni_{0.25}Co_{0.10}Mn_{0.65}O_{2.20}$ (or $Li_{1.000}Ni_{0.250}Co_{0.100}Mn_{0.650}O_2$)
$Li_{0.80}Ni_{0.25}Co_{0.10}Mn_{0.65}O_{2.10}$ (or $Li_{0.889}Ni_{0.278}Co_{0.111}Mn_{0.722}O_2$)

The chemical formula in the parenthesis is the layered structure nomenclature of solid solution. The mixed powders were then calcined at 900 °C for 10 h in flowing air.

2.2. Instrumental characterization

The crystal structures of the powder samples were determined by synchrotron HRPD performed at 9B HRPD beamline at Pohang Light Source II (PLS-II, Pohang, Korea) using the wavelength λ = 1.486 Å. The data were refined using the FULLPROF program. XANES and EXAFS measurements were carried at 7D-XAFS beamline in Pohang Accelerator Laboratory, Korea. The XANES and EXAFS data were analyzed by established methods using the ATHENA software package [33]. Morphology changes of the powders were determined using SEM (S-4700N, Hitachi). The inductively coupled plasma technique (ICP-AES) was used to determine the ratios of Li, Ni, Co, and Mn elements in each sample. In order to observe the transition metal distributions in the secondary particles, cross sections of the powder particles were prepared by Ar ion milling on a LN2 cooled stage and measured by an Electron Probe Micro-Analyzer (EPMA, JEOL JXA-8530F). The atomic-level structure and local phases were identified by diffraction and high-resolution TEM (FEI, Titan-cubed 60–300).

2.3. Computational methods

The first principle calculations were performed using the Vienna ab initio simulation package (VASP) [34,35] with the Projector-Augmented-Wave (PAW) method [36]. The exchange correlation interactions were included with the generalized gradient approximation Perdew-Burke-Ernzerhof (GGA-PBE) functional [37], and the plane wave cutoff energy was set to 500 eV. The structure relaxations were carried out with a criteria of 10^{-4} eV for the total energy, and 0.02 eV/Å for the forces on each atom. The effective on-site Hubbard U_{eff} corrections were 6.885, 5.95 and 5.0 eV on the 3d electrons for Ni, Co and Mn atoms, respectively [38]. The supercells selected in this work contained between 8 and 28 unit cells, depending on the sample composition and structure.

2.4. Electrochemical measurement

The electrodes were prepared by making a slurry of 92 wt% active material ($Li_xNi_{0.25}Co_{0.10}Mn_{0.65}O_{(3.4\ +\ x)\ /\ 2}$), 4 wt% conductive Denka Black, and 4 wt% polyvinylidene difluoride (PVDF) binder in *N*-methyl-2-pyrrolidone (NMP) as a solvent. The slurry was coated using doctor-blade method onto Al foil as a current collector. The electrodes

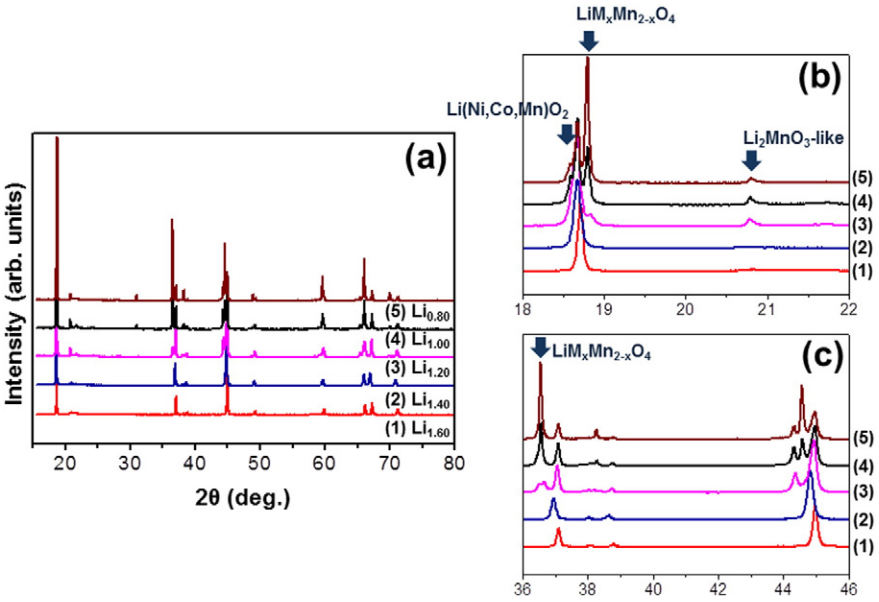

Fig. 1. (a) Panels (1)–(5) are XRD patterns of $Li_{1.60}$, $Li_{1.40}$, $Li_{1.20}$, $Li_{1.00}$ and $Li_{0.80}$ respectively, after heat-treatment at 900 °C. Selected angular ranges highlight the (b) layered and (c) spinel peaks.